TRIASSIC AND CENOZOIC PALAEOBIOGEOGRAPHY: TWO CASE STUDIES IN QUANTITATIVE MODELLING USING IDL®

Arnaud Brayard, Marie-Anne Héran, Loïc Costeur, and Gilles Escarguel

ABSTRACT

This work presents two examples of palaeobiogeographic reconstruction using the Interactive Data Language® (IDL). Although this meta-language is devoted to geoscientists and offers an array of easily usable tools, few palaeontologists actually use it. Our purpose is to illustrate how the IDL can be used to generate clear and direct visualizations of simulation results and interpolation methods for personal Geographic Information Systems (GIS).

The first example is a paleogeographic simulation of the biodiversity evolution of planktonic species (and especially ammonoids) in the Early Triassic. Principal results of this global scale simulation are that the formation of a marine latitudinal gradient of species richness depends on the shape and magnitude of the Sea Surface Temperature (SST) gradient, and the geographic location of the group's ancestor. Thus, the recovery pattern of Early Triassic ammonoids species richness can be simulated and explained by a general increasing trend in steepness of the SST gradient.

The second example describes a custom-designed GIS for large European Neogene continental mammals. Species richness and ecomorphologic parameters are interpolated, monitored in several ways, and discussed. Comparisons with the present-day distribution of large European mammals are also drawn and allow us to recognize that a broad North/South aridity gradient already existed by the Late Miocene with more open environments in Southern Europe.

Arnaud Brayard. Paläontologisches Institut und Museum der Universität Zürich, Karl-Schmid Strasse 4, CH-8006 Zürich, Switzerland and UMR-5125 CNRS, Paléoenvironnements et Paléobiosphère, Université Claude Bernard Lyon 1, 2 rue Dubois, F-69622 Villeurbanne Cedex, France
Arnaud.Brayard@univ-lyon1.fr
Marie-Anne Héran. UMR-5125 CNRS, Paléoenvironnements et Paléobiosphère, Université Claude Bernard Lyon 1, 2 rue Dubois, F-69622 Villeurbanne Cedex, France. marie-anne.heran@univ-lyon1.fr
Loïc Costeur. UMR-5125 CNRS, Paléoenvironnements et Paléobiosphère, Université Claude Bernard Lyon 1, 2 rue Dubois, F-69622 Villeurbanne Cedex, France. loic.costeur@univ-lyon1.fr
Gilles Escarguel. UMR-5125 CNRS, Paléoenvironnements et Paléobiosphère, Université Claude Bernard Lyon 1, 2 rue Dubois, F-69622 Villeurbanne Cedex, France. gilles.escarguel@univ-lyon1.fr

INTRODUCTION

The field naturalist vision is being increasingly abandoned in palaeontology, favouring desktop study ahead of fieldwork and leading to virtual palaeoworlds. Even though the numerical dimension may alienate scientists and disconnect them from the actual parameters of their problems, the use of numerical simulations can allow the testing of hypotheses that depend on multiple variables that putatively control the dynamic evolution of a system (Cleland 2001). Moreover, quantitative visualization offers illustrations or animations that may convey ideas more effectively. This paper investigates how powerful Interactive Data Language® (IDL) tools can be used to interactively visualize, analyse, and discuss results from large palaeontological data sets.

This work presents two examples of palaeo-biogeographic reconstructions, one Triassic and one Cenozoic, using the IDL programming environment. We begin by examining the Triassic example, a general 2D palaeobiogeographic model based on the constrained spreading of random phylogenies (Brayard 2002). Simulations are carried out in the biogeographic, thermal, and ocean current setting of the Early Triassic. Modelled and present-day Pacific Ocean Sea Surface Temperatures (SST) and Sea Surface Currents (SSC) are applied to discuss the recovery and distribution of planktonic species following the Permo-Triassic crisis. In the second part, we focus on IDL's Geographic Information Systems (GIS) facilities that can be used to plot mammal diversity and ecomorphologic data on Neogene palaeogeographic maps.

Both models are written with IDL 5.2 and run on Windows 98 and XP, Unix/Linux, and MacOS systems. IDL represents a complete computing and programming system for interactive analysis and visualization of data sets (Marschallinger 2001). IDL is a programming meta-language implemented in ENVI (Environment for Visualizing Images®) by Research Systems Inc. This meta-language is especially dedicated to numerical analysis and 2D/3D image processing. Several pre-packaged graphic modules are able to interact with each other, giving IDL a major advantage in time required for application development compared with other, more popular languages like FORTRAN or C. Yet IDL keeps its compatibility with standard programming languages through specialized functions.

IDL allows the user to create custom procedures, functions, or applications using simple matrix representation without using explicit loop structures to process matrix data, further reducing development time. IDL also allows the creation of graphic user interfaces. Results can be viewed immediately after processing using many pre-packaged graphic tools. All IDL functions, additional functions, and examples can be downloaded on the Research Systems Inc. homepage (http://www.rsinc.com). An open-source clone (PyDL) of IDL is also developed in Python for Linux.

In geosciences, this language has been used primarily for satellite image analysis and 2D/3D object modelling in applications such as the spatiotemporal analysis of basin history. The use of IDL in palaeontology is still rare and usually limited to the reconstruction and analysis of fossil morphology (Marschallinger 2001). In this work, IDL is used as a tool for calculating and visualizing palaeobiogeographic maps. The palaeobiological implications of this study will not be discussed in great detail; rather we concentrate on the construction of the two models and the benefits of IDL.

EXAMPLE 1: A 2-D EVOLUTIONARY/ DISPERSAL PALAEOBIOGEOGRAPHIC RECONSTRUCTION OF EARLY TRIASSIC AMMONOIDS

Overview of the Geological and Palaeogeographic Context

Early Triassic palaeogeography is relatively simple, largely because continents were joined together in a single block known as Pangea. Pangea was surrounded by a wide ocean (Panthalassa) and partially bisected by the Tethys Sea (Elmi and Babin 1996). The Triassic was followed by the largest mass extinction ever at the Permo-Triassic boundary. During this crisis, more than

90% of marine species disappeared (Raup and Sepkoski 1982). The reef fauna was severely affected and during this period trilobites became extinct (Erwin 1993, 1994). The Early Triassic appears to have been marked by poorly diversified faunal communities, composed of mobile species and a high percentage of predators (Erwin 1998, 2001). The Permo-Triassic crisis is considered to be the Phanerozoic's most drastic reorganisation of ecosystems and animal diversity.

By the Late Permian latitudinal temperature gradients were steep, but, in the late Upper Permian and in the earliest Triassic (Griesbachian), latitudinal temperature gradients were warmer and weaker from the pole to the equator. This change can be inferred from both the fossil record and climatic simulations (Hotinski et al. 2001, Kidder and Worsley 2004). The evolution of the latitudinal temperature gradient during the rest of the Early Triassic (Dienerian, Smithian, and Spathian) is still poorly understood (Kidder and Worsley 2004). However, the recovery of marine and terrestrial organisms following the crisis was reached by the Spathian/Anisian boundary (Erwin and Pan 1996), indicating that the latitudinal temperature gradient probably shifted by that time, with colder temperatures at high latitudes.

Ammonoids were the most prominent marine group during the earliest Triassic (Kummel 1973; Tozer 1973), when they were cosmopolitan with few species. The situation changed through quick diversification and organisation into latitudinal gradients of species richness (Dagys 1988). The greatest biogeographic differentiation of ammonoid faunas was observed in the Spathian with high endemism in boreal ammonoids (Dagys 1997). There were no important palaeogeographic events during the Early Triassic, which makes it an appropriate period to study the climatic influence on the biodiversity of ammonoids or other marine organisms possessing at least one planktonic or pseudo-planktonic living stage. We used a numerical model of the Early Triassic palaeogeography, to simulate the redistribution of biodiversity and the evolution of planktonic or pseudo-planktonic organisms, in response to parameters such as SST, SSC, and speciation and extinction rates.

Algorithm

The probabilistic model presented below uses two physical environmental factors (SST and SSC) to control geographic displacements, speciation events, and extinction of planktonic species (Brayard 2002). We used an algorithm based on the idea of cellular automata. These automata are divided in modules interacting with each other via action or reaction loops. Depending on local conditions, numerical objects (e.g., cells, sand particles) can interact and self-organize, creating spatial and temporal patterns (Wootton 2001).

The program was designed in three parts (Figure 1). The main module built the Early Triassic palaeogeography from a digitized version of a published reconstruction (Smith et al. 1994, from 60° North and 60° South and from 180° West to 180° East, Figure 2). The geographic space is represented as an X * Y matrix corresponding to the longitudinal (X) and latitudinal (Y) subdivisions in which each grid-cell represents a quadrate of 360/X° by 120/Y°. Land is coded as 1 and sea as 0. The system also handled the biogeographic distribution of n simulated species whose presence (coded as number 1) or absence (coded as number 0) are saved in a matrix with dimensions X * Y * n, where n is the number of species.

The second module applied a latitudinal gradient of SST to the X * Y * n biogeographic matrix, which constrains geographic displacements, speciation events, and local extinctions for each simulated species based on a fixed or random thermal range for that species. Because the shape, intensity, and evolution of the SST gradient through the Early Triassic are actually unknown, we constructed a number of hypothetical SST gradients using the present-day Pacific gradient as a starting point (data from the National Oceanic and Atmospheric Administration http://polar.wwb.noaa.gov). Even if the Panthalassic Ocean was significantly wider than the modern Pacific, the choice of the Pacific SST gradient as a model is justified by the global geographic similarity between the two.

The third module managed the distribution, direction, and intensity of oceanic currents. The module is activated every time a species displacement on the biogeographic grid is called for. We also derived the Early Triassic current configuration from the present-day Pacific as represented in the current data published by Pickard and Emery (1990). The matrix of currents was constructed by choosing a single direction of current (among eight possible directions) for each cell. Each direction was coded by a number from one to eight. Zero is equivalent to the lack of a current and therefore equal probability of displacement in any directions (Figure 3). Current intensity was represented using discrete probabilities of displacements – the higher the probability in one direction, the higher the strength of the current (Figure 3). Use of continuous probabilities (e.g., calculated from equations of diffusion and advection) would make the displacements more realistic; nevertheless, it would involve
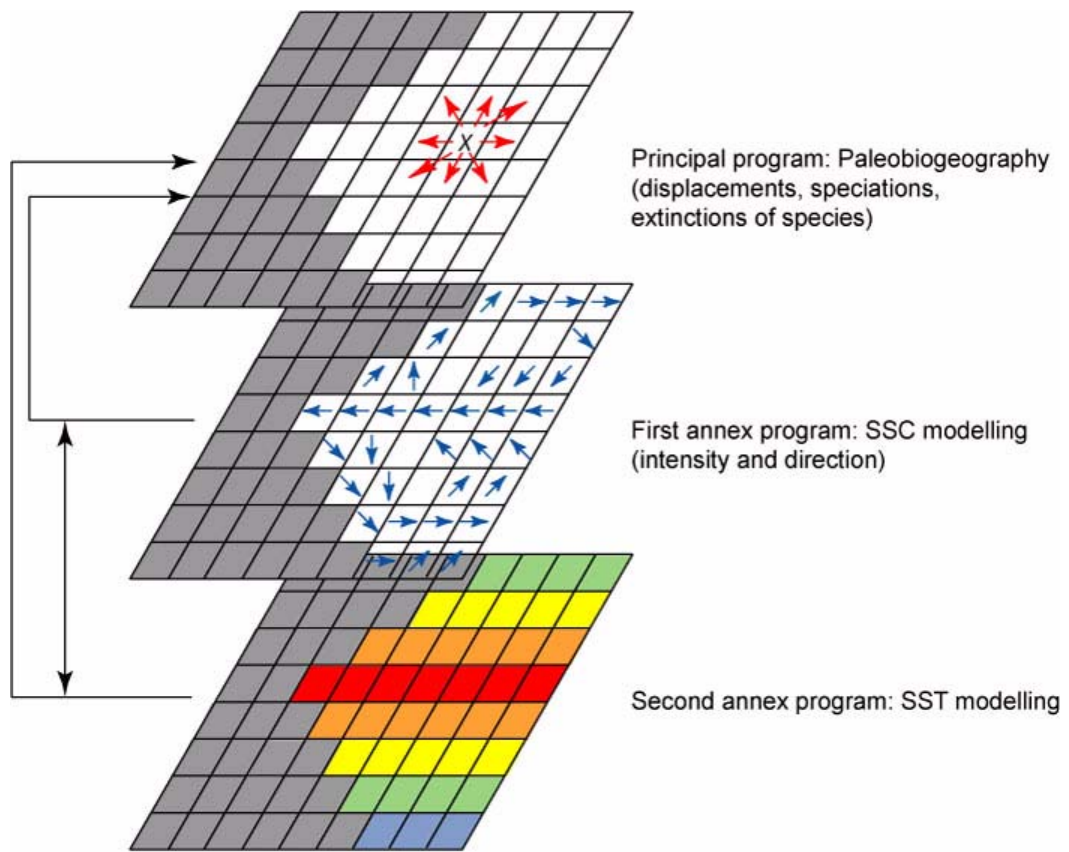
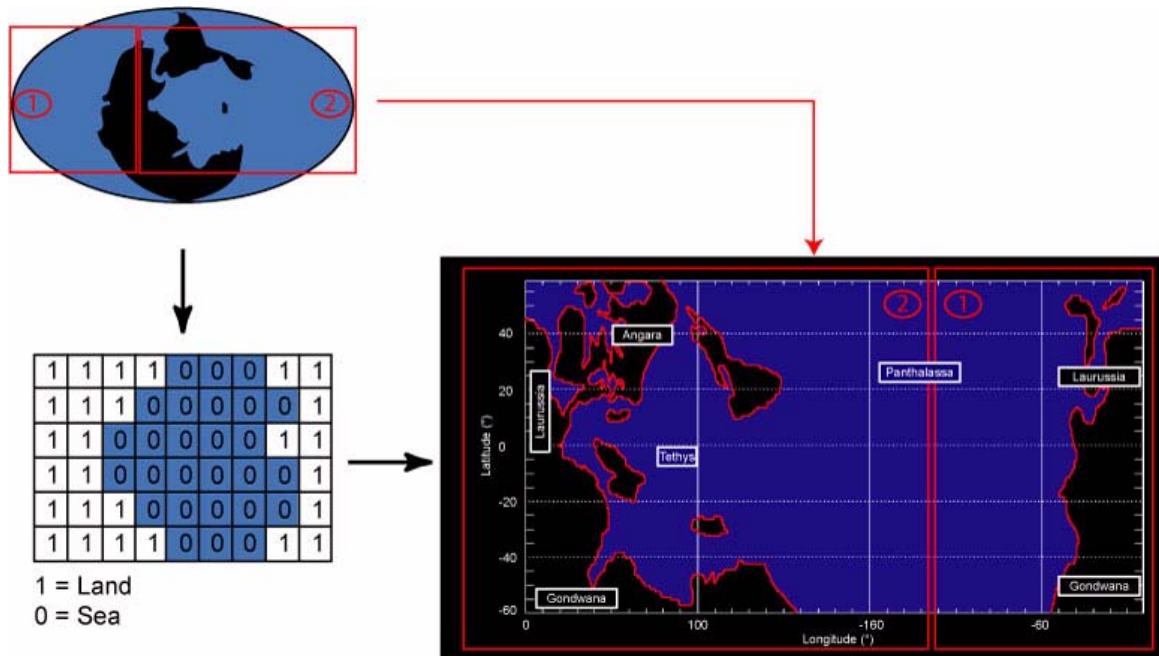**Figure 1.** Simplified algorithm decomposed in three principle parts.

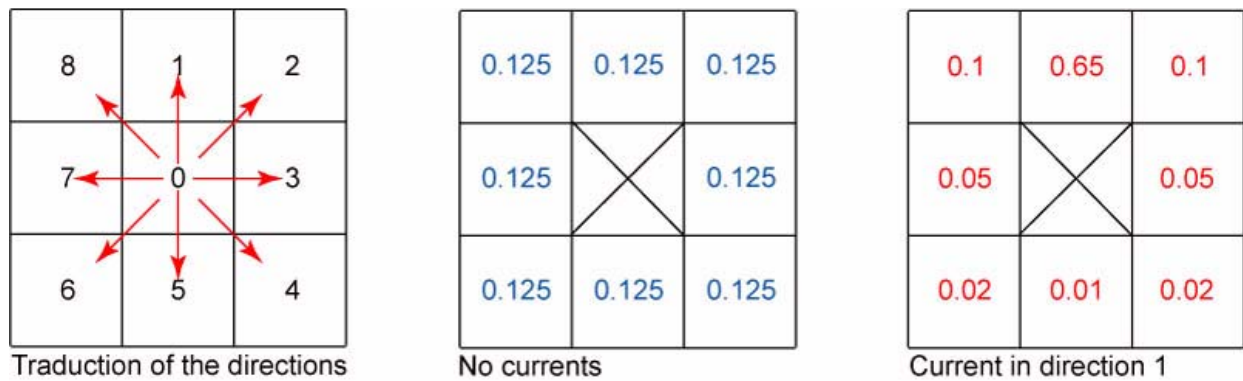**Figure 2.** Construction of the Early Triassic palaeogeographic map based on Smith et al. (1994).

Figure 3. Probabilities of displacements for a simulation without currents and another with a current in the direction 1.
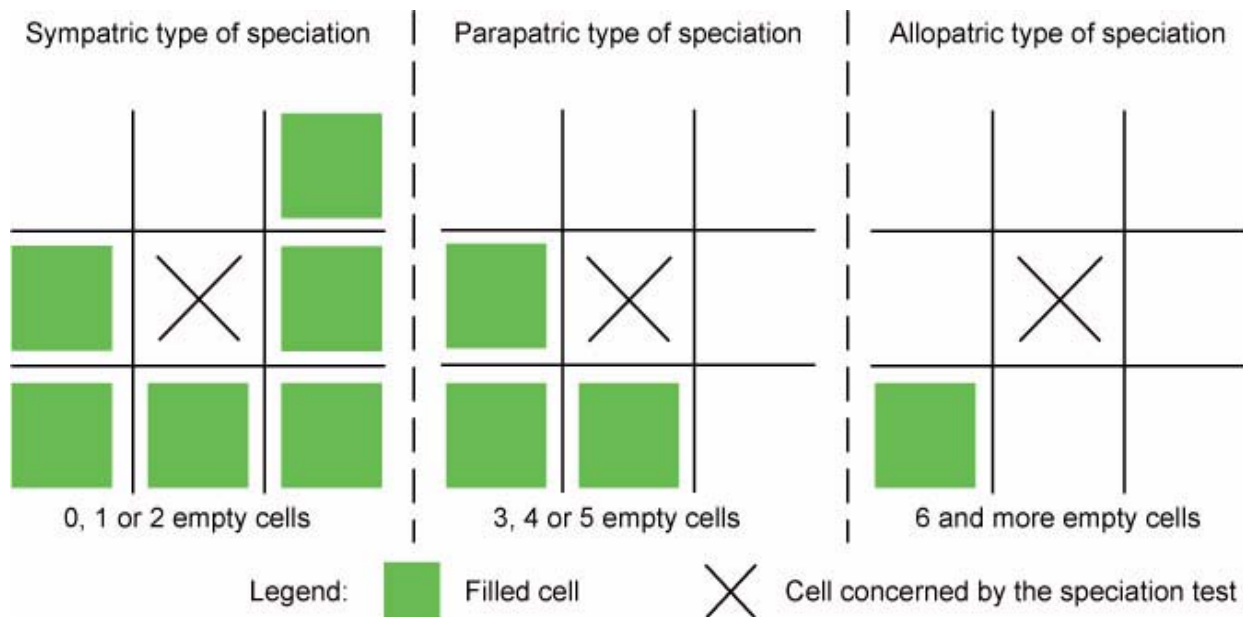

Figure 4. Quantification process of the geographic isolation of a simulated species and corresponding speciation type.

serious complications in computation without affecting the broader-scale simulation results.

The algorithm of the program can be divided in five successive steps where our parameters are successively tested:

1. Speciation: Given a fixed probability of speciation, a new species can be created in a cell occupied by its "parent-species." Three types of speciation events were distinguished: sympatric, parapatric, and allopatric, each with its own probability of occurrence. The type of speciation depended on the number and location of adjacent filled cells (Figure 4). Speciation probability and number of surrounding filled cells were inversely correlated. A species was added (cladogenesis) to the biogeographic matrix in the form of a supplementary layer by extending the n-dimension (Figure 5).

2. Displacement: A species occupying a cell can move to surrounding cells only if those cells are not already filled with the same species, and only if displacements in that direction are allowed by the superimposed oceanic currents. The module managed displacements in four successive steps in which first current direction, then intensity, then species displacement direction, and finally displacement success were determined (Figure 6).

3. Extinction: Two cases were distinguished: "local" and "complete" extinction, each having its own probability of occurrence. A species extinction in a filled cell ("local" extinction) did not affect the neighbouring cell filled with this species. In the case of a "complete" extinc-
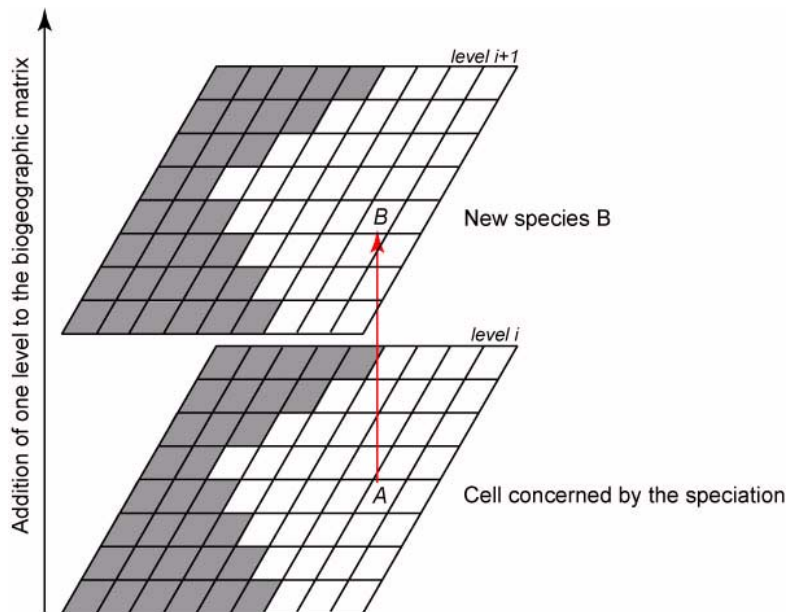
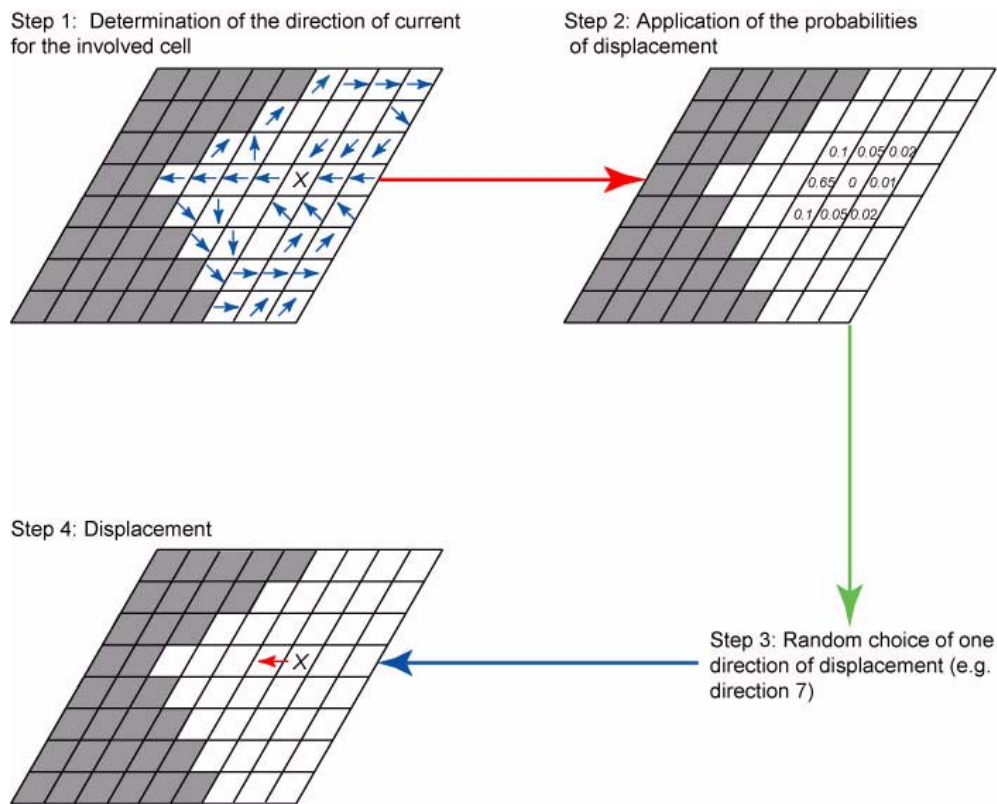**Figure 5.** Illustration of a speciation event.

Figure 6. Illustration of how current displacement is modelled.

tion, all cells filled with the same species are simultaneously emptied.

4. Diversity check: The program checked for cells whose diversity threshold has been reached to avoid an ecologically unrealistic accumulation of species (Figure 7).

5. Species richness monitoring: Finally, the program calculated the species richness for each cell as the sum of co-occurring species.

Even if these five steps are successively executed for each cell and time iteration, speciation, extinction, and displacement events do not neces-
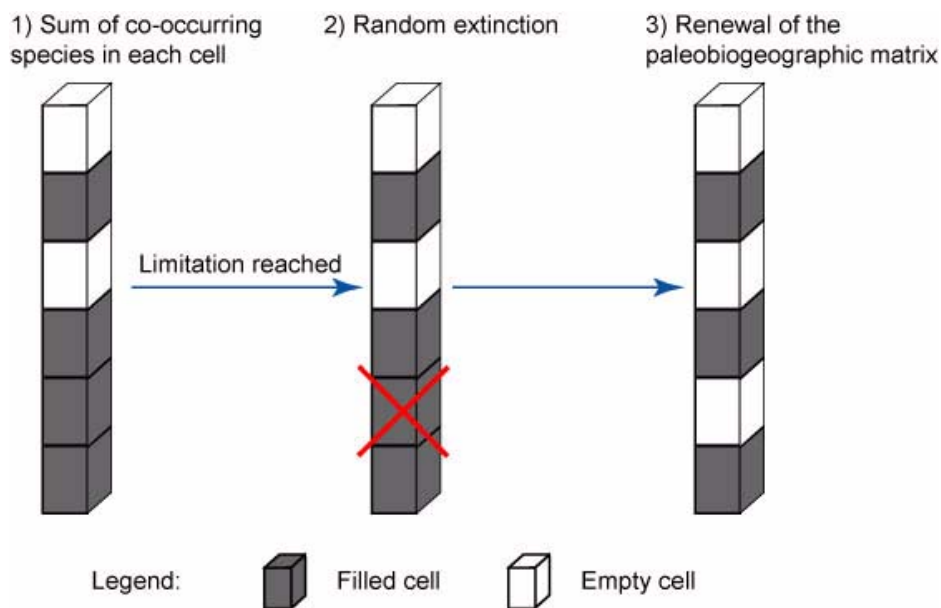
Figure 7. Limitation of the species richness in one cell given a threshold of co-occurring species.

sarily occur. As a result, the evolutionary rate of each cell is independent from cell to cell.

Results

Running our model for several hundred iterations (depending on the SST gradient and the selected speciation and extinction rates) allows us to construct theoretical patterns of species richness distribution under SST and SSC constraints. These theoretical patterns can be compared to the real ones observed in Early Triassic ammonoids.

Simulation Running without Currents and with a Weak SST Gradient. As a benchmark, we ran a simulation with no SSC and only a weak SST gradient, implying a weak or nil latitudinal and/or longitudinal bias in the geographic distribution of the simulated species. The results represent a random and thus statistically homogeneous distribution of the simulated species (Figure 8): simulated species are logically not organized along a diversity gradient. This example may correspond to the wide palaeogeographic distribution of the first earliest Triassic invertebrate marine species (like the two surviving ammonoid genera *Otoceras* or *Ophiceras*, *Lingula* for brachiopods or *Claria* for bivalves; Kummel 1973, Erwin and Pan 1996). This null model suggests that the SST gradient strongly influences the emergence and the general structure of a latitudinal gradient of species richness (LGSR).

Impacts of Currents on the Simulation. In order to visualize the impact of currents, we can apply them fully, partially, or not at all. If we impose

no diffusion and only transport in the direction of the current, the species is destined to stay in the oceanic gyres for many iterations, but if we allow both diffusion and transport in the direction of the current, species are distributed along the principal currents, as well as in intermediate zones (Figure 9.1-4). Our simulations indicate that currents have a strong influence only over the timing (especially on the dispersal throughout the Panthalassa) and local patterns of dispersion of the simulated species. They have no influence on the shape and magnitude of the simulated LGSR on a global scale. If we remove currents from the simulation, the general shape and magnitude of the LGSR is conserved. Mixed water assemblages driven by currents do not seem to be the preponderant factor for explaining patterns of low species diversity in some convergence zones (e.g., equatorial, contra Casey 1989; Rutherford et al. 1999; Kiessling 2002).

Simulations with the Present-Day SST Gradient. If we apply the present-day SST gradient to the model, we might expect a LGSR similar to the classical view of species richness increasing monotonically and regularly from the poles to the equator. This pattern has been recognized in terrestrial and marine environments and for faunas and floras from all geological time periods (Stehli et al. 1969; Schopf 1970; Rex et al. 1993; Gaston 2000; Crame 2002; see also Rhodes 1992 for a review of hypotheses about the formation of latitudinal gradients in species richness).
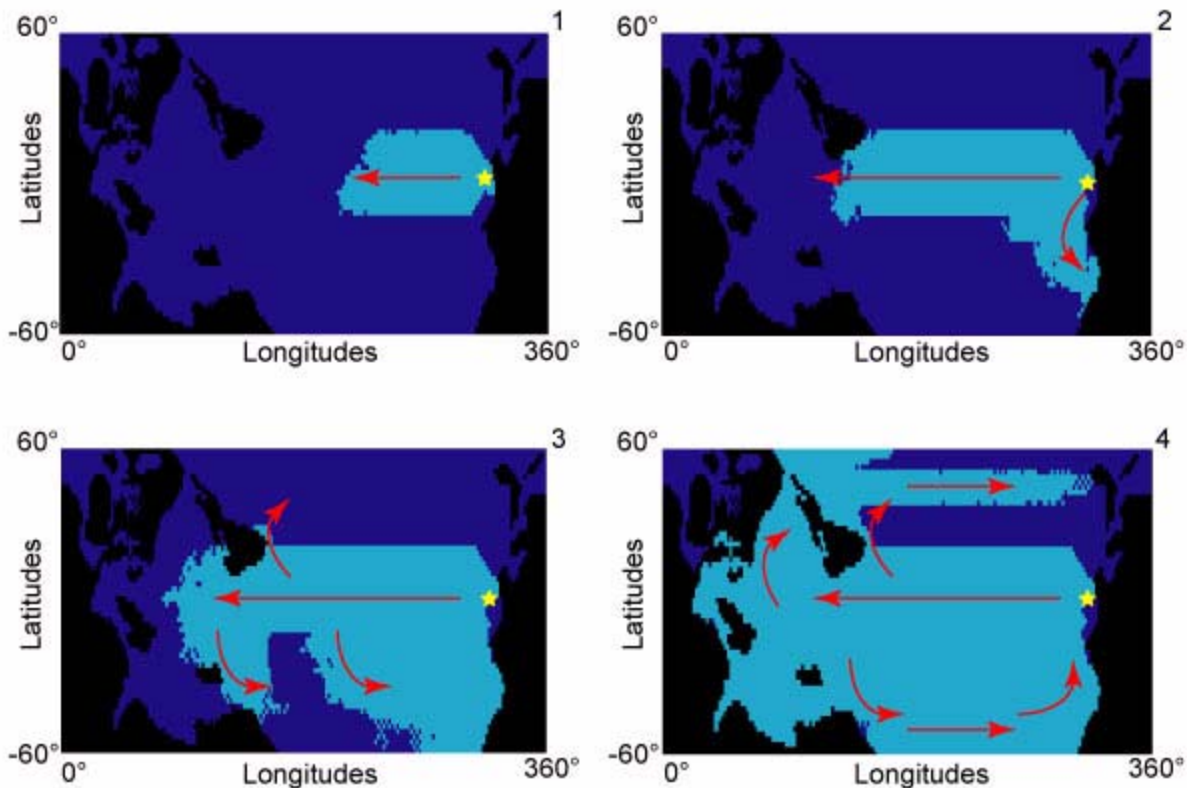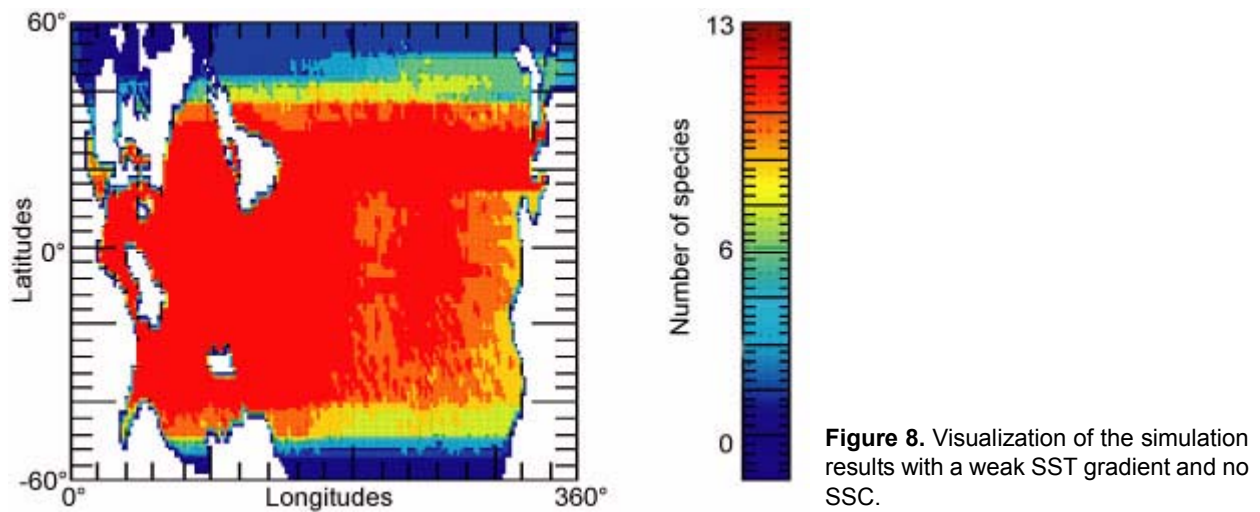
Figure 8. Visualization of the simulation results with a weak SST gradient and no SSC.

Figure 9. Example of a simulated species not sensitive to temperatures, spreading from the West coast of Pangea throughout the Panthalassic Ocean. The yellow star indicates the position of the species origination.

However, our results suggest a quite different pattern with a slight decrease in species richness near the equator (Figure 10.1). In fact, most of the simulations found maximal species richnesses close to the Tropics of Cancer and Capricorn. This pattern results from the geometric overlap of the species distributions as influenced by the shape and intensity of the SST gradient (Figure 11). This by-product of superimposed thermal ranges has been described in the modern setting as the "mid-domain effect" (Colwell and Hurtt 1994, Colwell and Lees, 2000, Colwell et al. 2004). This principle suggests that observed LGSR may simply be the result of chance. In situations with two fixed boundaries, randomly distributed ranges never generate a uniform spatial distribution but always
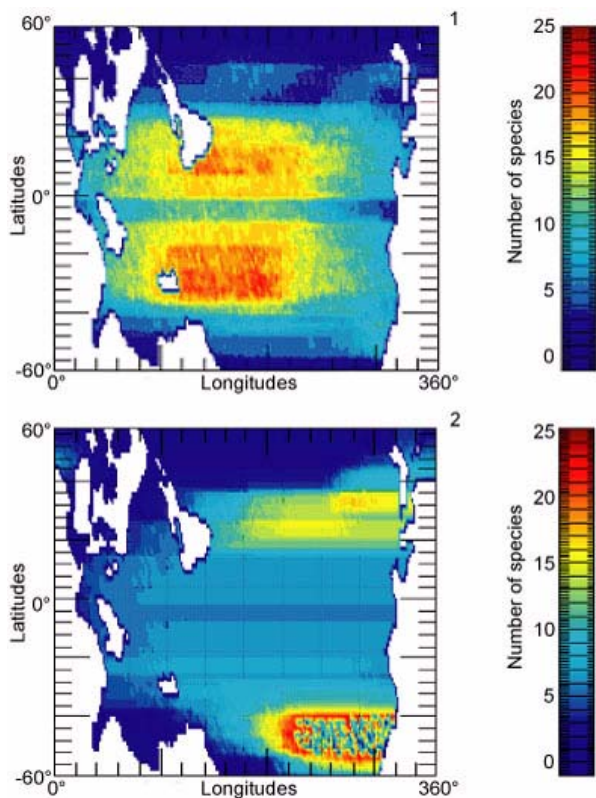
Figure 10. Visualization of the simulation results 1) with a present-day SST gradient 2) with a present-day SST gradient and first simulated species originated in middle/high latitudes (50°N).

give rise to a peak or a plateau of species richness. In the absence of any environmental or historical gradients, the formation of an LGSR may be solely the consequence of the spatial distribution of the thermal ranges of species as controlled by the SST gradient. If we change the SST gradient, the LGSR also changes (Figure 8). If a change takes place in the thermal ranges of species or in the position of the ancestral species, the LGSR is immediately affected (example in Figure 10.2).

Our simulation thus indicates that the formation of a gradient of taxonomic richness for marine organisms with at least one planktonic or pseudo-planktonic stage can be partially, if not completely due to: 1) the superimposition of species thermal ranges according to the geometry of the SST gradient; 2) the evolutionary history of the taxa (latitudinal position of the lineage origination); and 3) the characteristic parameters of individual species affecting the local species distribution.

Simulation of a Changing SST Gradient Applied to the Early Triassic. The SST gradient can be changed at any given iteration of a simulation. When a simulation starts with the present-day SST gradient and then a weak SST gradient is applied, the species distribution becomes homogenized and cosmopolitan. Species whose thermal range excludes them from the coldest temperatures disappear. When we change the SST gradi-
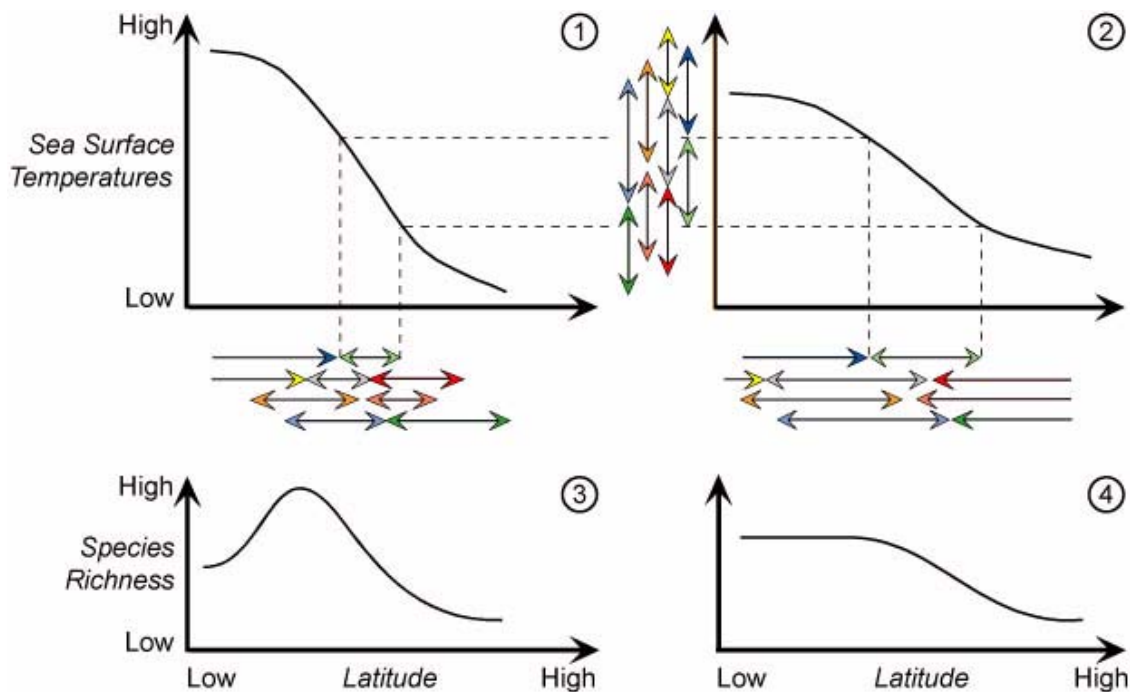

Figure 11. Illustration of the causal effect of the magnitude of the SST gradient on the shape and magnitude of the resulting LGSR. The latitudinal projection (horizontal arrows) of a given random distribution of thermal ranges (vertical arrows) on a steep (1) or weakened (2) SST gradient leads to a steep bimodal (3) or weakened unimodal (4) LGSR, respectively.
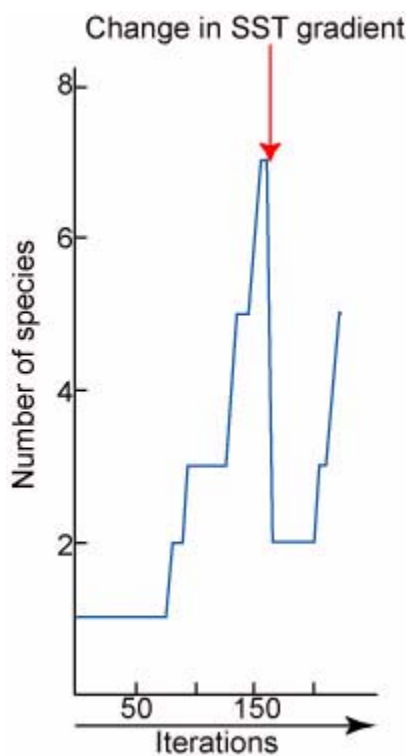
Figure 12. Illustration of the drop in species richness when an abrupt increase of the SST gradient occurs.

ent to be warmer and weaker, only tropical species survive after which they colonize higher latitudes. However, with a colder, weaker SST gradient, only high latitudes species survive and progressively invade low latitudes. If we proceed in reverse, set-

ting a weak SST gradient at the start and abruptly changing it to a very steep one, we obtain a drop in the total species richness (Figure 12).

All thermal variations yield disruptions in species richness. On a global scale, this type of simulation can easily represent climatic changes in time and space and their consequences on the distribution of species on Earth. Changes of the SST gradient during the simulation evoke changes that reproduce observed diversity curves. For example, in Figure 13 we identified a sequence of changes to the SST gradient that can be hypothesized to have occurred during the Early Triassic. The SST parameters of the program were iteratively constrained to produce a species richness curve that maximally corresponds to the real diversity curve. The beginning of the simulation corresponds to the weak and warm pole-to-equator SST gradient of the Permo-Triassic boundary. Principal observations are: 1) a lowering of the SST gradient corresponds to a decreasing of endemism; 2) a steepening of the SST gradient leads to an increase of latitudinally restricted taxa.

The recovery of ammonoids after the Permo-Triassic extinction was not a continuous increase in species richness (Figure 13) or of the steepness of the LGSR, but was a sequence of increases and decreases. These fluctuations also differed latitudinally. In spite of their geographic complexity, our simulation indicates that the fluctuations of species richness can easily be modelled with simple changes in the SST gradient, which strongly sug-
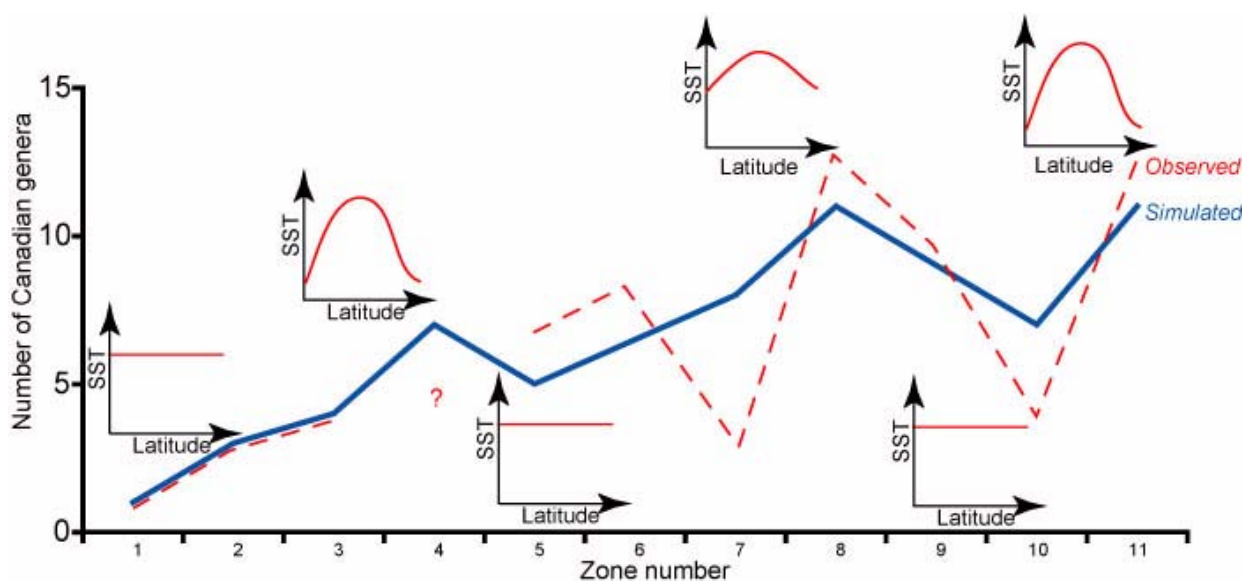

Figure 13. Evolution of the Canadian ammonoid generic richness (middle palaeolatitudes) during the Early Triassic (based on Tozer [1994] and unpublished data) and possible corresponding evolution of the SST gradient as suggested by our simulation results. Zone numbers correspond to the Canadian ammonoid zonation by Tozer (1994).

10

gests that such SST gradient directly influences the marine species richness and its distribution on Earth.

It appears that the formation of global-scale marine LGSR may be due to the shape and magnitude of the SST gradient, and to the location of the ancestral species. Even if it seems problematic to invoke only a single biotic (e.g., physiologic) and/or abiotic (physical environment) factor, the origin of the latitudinal species richness gradient can be the simple geometric by-product of the geographic overlap of thermally constrained species ranges. Through our model, IDL improved the visual understanding of the consequences of a changing climate on the distribution of species. IDL is completely adapted to run and visualize biogeographic models with an evolutionary time dimension.

EXAMPLE 2: BIODIVERSITY AND PALAEOENVIRONMENTAL INTERPOLATED BIOGEOGRAPHIC MAPS OF EUROPEAN NEOGENE LARGE LAND MAMMAL FAUNAS

The following example shows how the Interactive Data Language can be used to model biodiversity and ecomorphologic proxies in the European Neogene geographic context.

The European continental Neogene has yielded hundreds of localities containing mammal remains. This important collection of data is now being used to study the evolution of biodiversity (Fortelius et al. 1996, Costeur et al. in press) and palaeoecology of the mammalian communities (Fortelius et al. 1996, Van Dam and Weltje 1999, Fortelius et al. 2002, Jernvall and Fortelius 2002). The different studies cited above have brought to light different large scale or regional patterns linked to climatic and/or geographic evolution in large or small mammal faunas. Our purpose here was twofold. First, we investigated the large mammal species geographic distribution in relation to the Neogene palaeogeography. Second, we used ecomorphologic parameters to characterize large mammal communities on a taxon-free (Damuth 1992) ecological basis in order to infer past environments.

Palaeogeographic maps of the Neogene have been suggested (Rögl 1999, Meulenkamp and Sissingh 2003) but few biodiversity and/or palaeoecological studies have attempted to represent classical analysis results on maps. The IDL metalanguage and its representation facilities offer the opportunity to investigate biogeographic and environmental patterns resulting from the analysis of mammalian communities with direct visualizations onto palaeogeographic maps.

Data

Two different datasets were used. The first was a collection of extant European large mammals (data from Legendre 1989 and unpublished, and Héran unpublished), which was be used to test IDL interpolation functions. Comparisons of the results with recent studies on the distribution of land mammals (Baquero and Telleria 2001) provided information on the reliability of the IDL tool.

The second dataset was a compilation of 100 Tortonian European localities that have yielded large fossil mammals (Costeur unpublished). Their presence/absence as well as different ecomorphologic parameters (e.g., hypsodonty, tooth crown height) were recorded and evaluated. We used these to produce palaeobiogeographic maps of the distribution of species richness and of environmental proxies such as humidity/aridity. Palinspastic palaeogeographic backgrounds were built from published maps (Rögl 1999, Meulenkamp and Sissingh 2003), and their settings will be explained in the next section. Spatiotemporal coordinates for each locality were amalgamated from their ages and present-day latitude and longitude.

Algorithm

The algorithm used here was simpler than in the simulation of Triassic species richness. The algorithm was built in three steps.

Step One: Data Acquisition.

1. Palaeogeographic maps were generated as before using Tortonian and Recent maps of Europe and North Africa. The first step was to load the map into a corresponding 60 x 100 binary matrix (zero for oceanic areas, one for continental areas; see Figure 2 for an overview of the process). Each map covered the area between 30° North to 59.5° North and 10° West to 39.5° East. Each cell of the matrix thus represented an area of 0.5° x 0.5° corresponding to a mean surface of ca. 2200 km.

2. Faunal data: Locality characteristics (palaeogeographic coordinates and values to be interpolated) were read by the program from a text file provided by the user.

Step Two: Interpolation.

Our program offers two interpolation methods from among those included in the IDL library: Delaunay triangulation and Thin Plate Spline (TPS; Yu 2001). Sugihara and Inagaki (1995) described the Delaunay triangulation method. We will not dis-
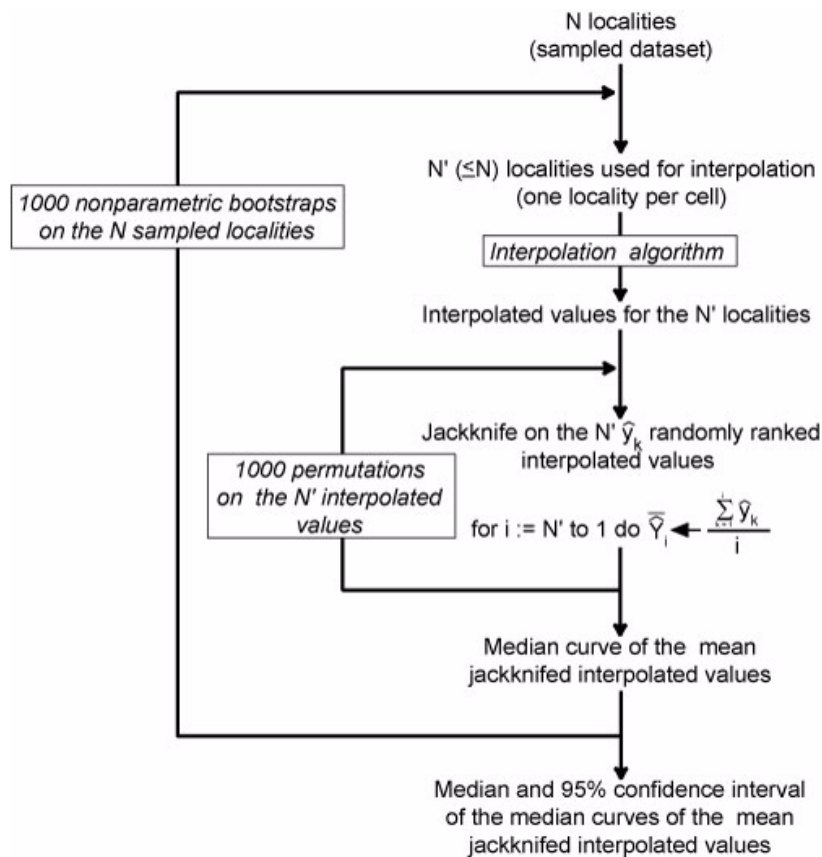
Figure 14. Flowchart illustrating the three nested levels of the "quality" test algorithm for an interpolation method.

cuss the mathematical foundations of these techniques here, but the basis for this interpolation method is to construct connected triangles between the data points and use them to determine unknown values by calculating a regression between their vertices. Thin Plate Splines apply a tight surface using a smooth bivariate function that takes the data points into account and assumes a minimum curvature of the surface (Monnet et al. 2003).

Other interpolation methods exist, including the popular Kriging-Cokriging method (Boer et al. 2001). Even though the Kriging algorithm is implemented as a routine in IDL, we did not use it because of the high subjectivity needed to choose the parameters that best fit the variogram, and because it is a computationally difficult method that requires an extensive practical experience compared to TPS and Delaunay triangulation.

TPS and Delaunay triangulation interpolate on a gridded geographic matrix so locality data provided by the user were placed in a matrix of the same dimensions as the palaeogeographic one (i.e., within cells of 0.5° x 0.5°). If more than one locality falls into the same cell, which is often the case with coarse resolution, several choices are proffered. Depending on the needs of the investigation, the minimum, maximum, mean, or median

value of the parameter can be computed. The interpolation is then conducted on the matrix generated from the computed values. The computation does not distinguish coastal boundaries; a "continent" filter is later applied for visualization.

Step Three: Output.

A twofold sub-routine allows the validity of the results to be tested:

1. We first evaluated the "quality" of the interpolation results; for example, testing whether the dataset is large enough to yield a stable mean interpolated value regardless of the spatial distribution of the samples. To do this, we performed an analysis similar to a standard rarefaction procedure in which the relationship between the size of the set localities and the mean interpolated value was assessed. An algorithm involving three nested levels was applied (Figure 14):
   • The innermost level is a jackknife applied on the N' interpolated values associated with the sampled cells (N' ≤ N sampled localities because several sampled localities can be located in the same geographic cell). The resulting curve is made of N' mean interpolated values; it depends on the (arbitrary) order by which the N' inter-

polated values were successively removed.

- The second level was a random permutation of the N' interpolated values to randomize the removal order of the jackknife, which results in a median jackknifed curve which is independent of the removal order of the interpolated values, but still depends on the N sampled values;.

- The third level is a nonparametric bootstrap (random re-sampling with replacement) applied on the N sampled localities in order to estimate the median and confidence interval associated with the mean interpolated value parameter. The resulting relationship (and its associated bootstrapped confidence interval) between the number of localities and the mean interpolated value strongly depends on the shape of the distribution of the interpolated variable, and thus illustrates an important statistical characteristic of the interpolation method that was used.

2. We then tested the reliability of the TPS-interpolated values by computing the correlation coefficient between observed and predicted values (Monnet et al. 2003). This second test is obviously meaningless in the case of the Delaunay triangulation as the interpolated values for the sampled localities are the observed ones by definition of the method.

Results

We tested the reliability of the IDL tool on the present-day distribution of large European mammal species richness. We interpolated species richness across Europe from 151 evenly distributed sampling points using Delaunay triangulation and TPS (Figure 15).

Species richness is highest in Central Europe and decreases toward coastal areas as already demonstrated by Baquero and Telleria (2001). Those authors indicated that this pattern is consistent with a peninsular effect and decreasing land areas toward the borders as well as with the environmental parameters that prevail on the study area and the historical factors that affected Europe during the Quaternary. Both interpolation methods produced this same general pattern.

We then investigated the link between present-day environmental variables and the distribution of species throughout Europe by means of direct comparisons between plots of morphologic characters related to the animals' ecology and plots of diverse environmental variables. Such comparisons for present-day faunas would serve as a basis for relating large Neogene mammals to their environment.

Each species was assigned to a dental crown height class: brachydont (1), mesodont (2), or hypsodont (3) when their teeth possessed low, intermediate, or high crowns, respectively (Fortelius et al. 2002). Each dental crown height class characterizes a particular type of diet, from one dominated by non-abrasive plants (mostly found in rather closed and humid environments) to one dominated by highly abrasive plants (mostly found in open and arid environments; Fortelius and Solounias 2000). Mean dental crown height was calculated across species for each locality. Figure 16 shows Delaunay triangulation and TPS interpolations of the present-day mean dental crown height values, and Figures 17 and 18 present the quality of the interpolation methods (note that the bootstrapped median jackknifed curves are shorter than the observed one due to random re-sampling of the same sampled localities reducing the number N' of geographic cells involved in the interpolation). For both methods the bootstrap median of the median jackknifed mean interpolated values, and their associated 95% confidence intervals were remarkably constant, even for small-sized datasets. The negative bias that appeared with small-sized datasets (N' < 15 localities) is the logical consequence of the strongly right-skewed distribution of the mean hypsodonty values of the sampled localities. It is worth noting that the bootstrapped 95% confidence intervals estimated for the TPS method were wider than for the Delaunay triangulation method illustrating the greater sensitivity of the TPS algorithm to spatial heterogeneity of data.

Figure 16 depicts a broad North/South gradient with a few areas of higher tooth crown height in eastern Spain, southern France, Switzerland, and northeastern Italy. If we directly compare this map to the present-day precipitation and temperature interpolated maps (Delaunay Triangulation, Figure 19), we can associate the latitudinal differentiation with lower precipitation and higher temperature in the south, which is itself associated with more arid and open environments, thus explaining the hypsodonty maximum in that region. A multiple correlation analysis with temperature and precipitation as independent variables and hypsodonty as the dependent variable indicated a significant association: Pearson r = 0.522, bootstrapped (n = 10000) 99% Confidence Interval: 0.22 – 0.72; Mantel's t 0.0001 (n = 10000, H0 = no multi-linear association).
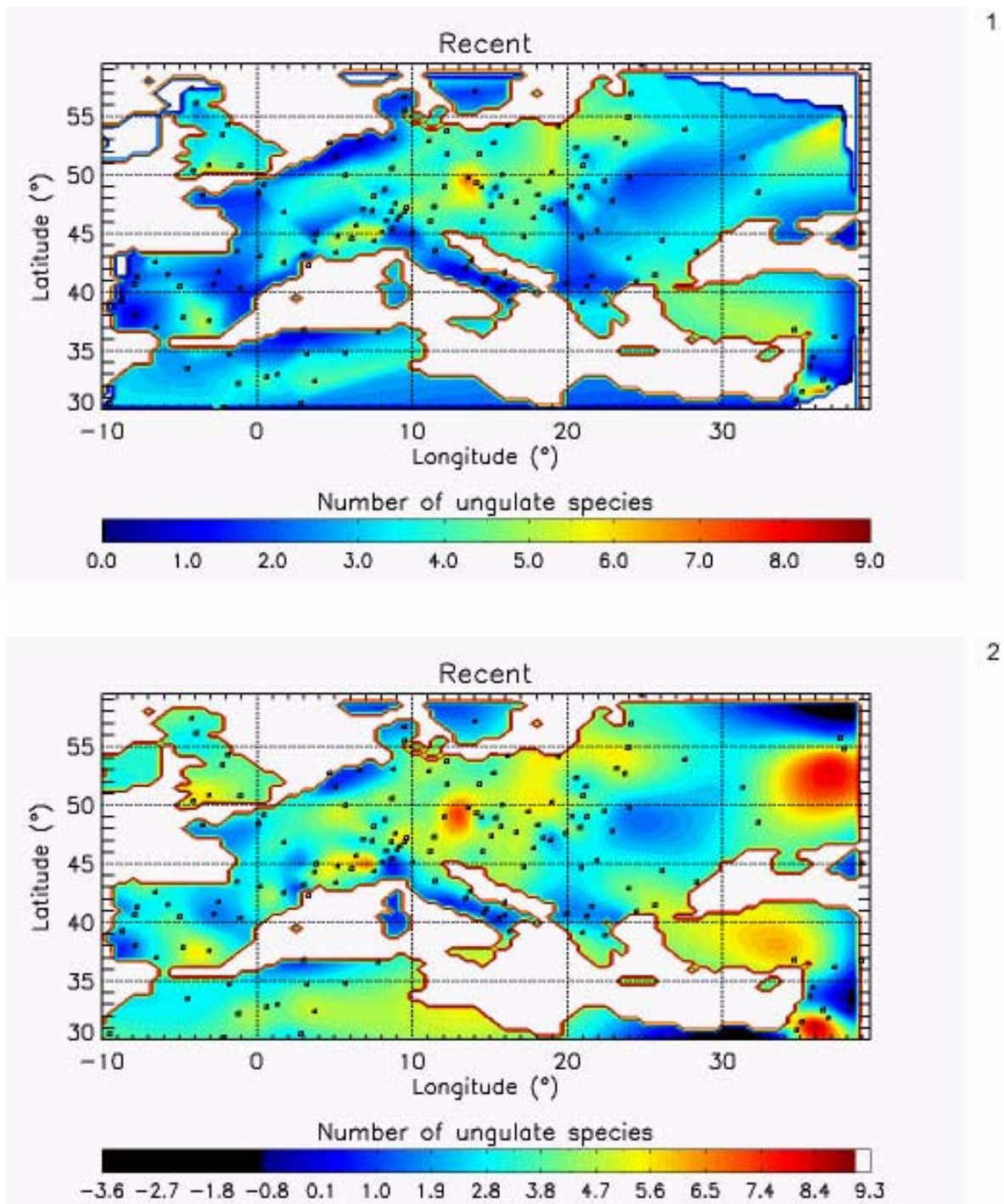
Figure 15. Present-day species richness of ungulates in Europe: 1) Delaunay triangulation interpolation, 2) TPS interpolation. Faunal locations are shown by open squares.

Once the link between climatic parameters and ecomorphologic parameters such as mean hypsodonty has been characterized, it is possible to use that relationship to interpolate a similar map for fossil data. Here we present an example for the large Tortonian mammals (the other Neogene continental stages have also been investigated in the same way). Figure 20 shows the hypsodonty pattern for 100 Tortonian sites distributed throughout Europe. We plotted the results onto a palaeogeographic map drawn from Rögl (1999) using palaeocoordinates calculated from present-day coordinates, as well as stratigraphic and geographic positions. Figures 21 and 22 show the quality of fit
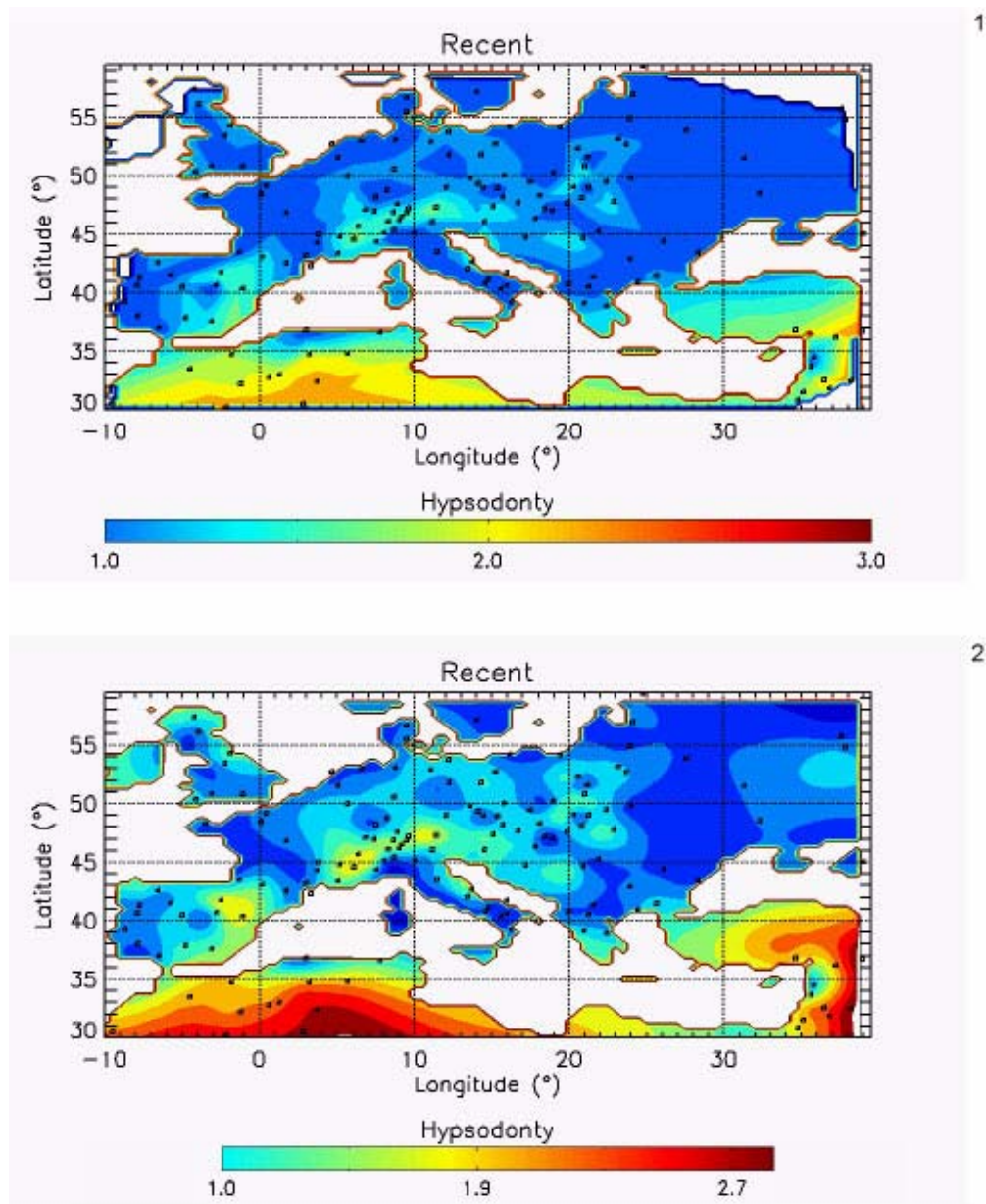
14

Figure 16. Present-day distribution of ungulates hypsodonty: 1) Delaunay triangulation interpolation, 2) TPS interpolation. Fauna locations are shown by open squares.

for Delaunay and TPS-interpolated data. As for the present-day data, the bootstrap median of the median jackknifed mean interpolated values and its associated 95% confidence interval were independent of the size of the analyzed dataset. Here the low skewness of the hypsodonty distribution makes the two interpolation methods immune to very small-sized dataset bias. As already mentioned, the TPS method showed a wider bootstrapped 95% confidence interval than the Delaunay method due to its greater sensitivity to spatial heterogeneity. Indeed, the fact that the bootstrapped median jackknifed curves were uniformly shifted upwards

for the TPS-interpolated Tortonian dataset indicates that this parameter is critical. Thus the TPS-interpolated values should be interpreted very cautiously.

The Tortonian hypsodonty pattern broadly shows a North/South gradient with the highest values being mainly concentrated in the Iberian Peninsula and in the Greek-Iranian block (Bonis et al. 1992). The central-eastern European localities (eastern France, Germany, Switzerland, Austria, and Romania) have lower mean values of tooth crown height. Note that the sharp decrease observed towards the northern boundary is an
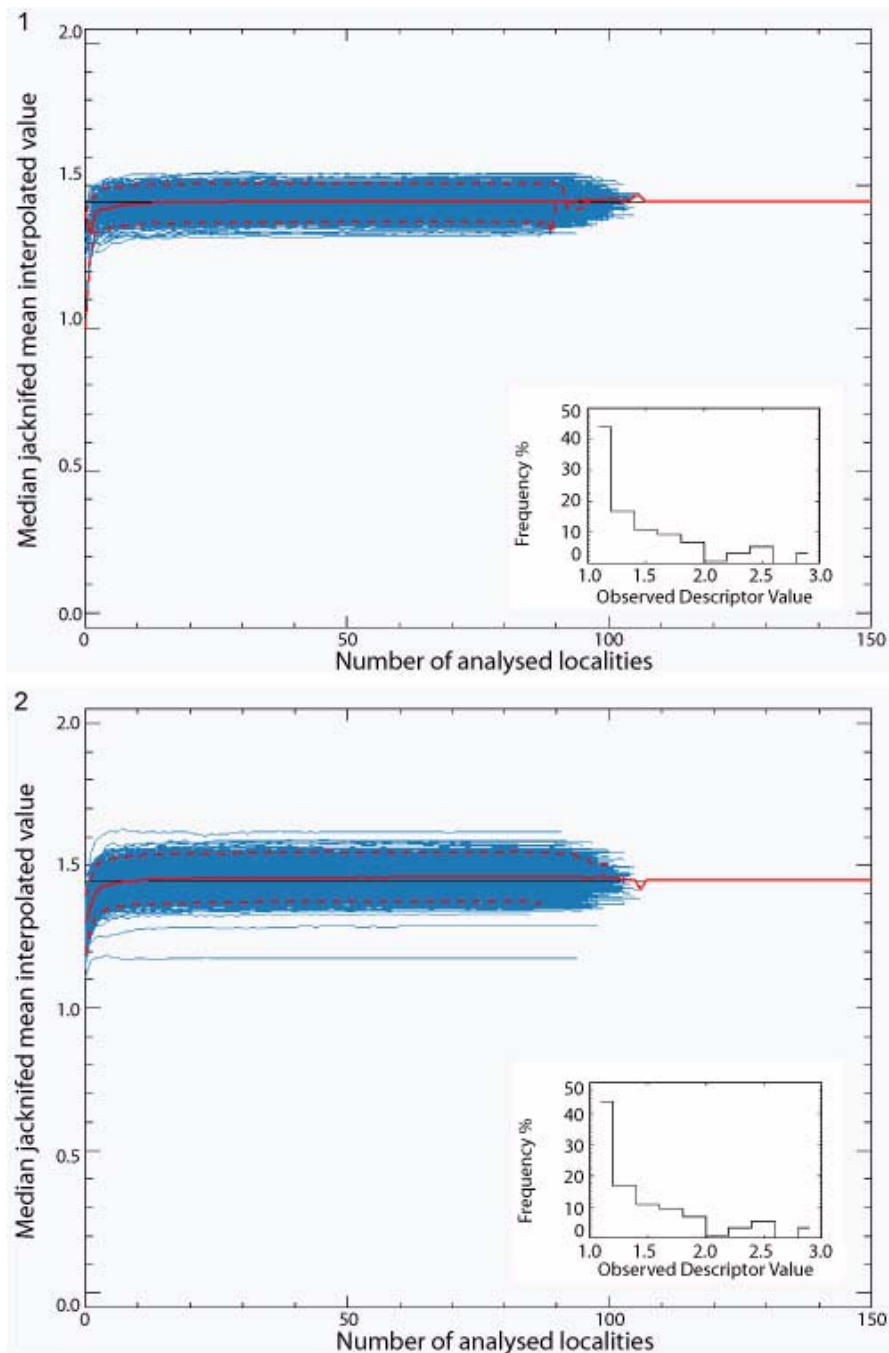
15

Figure 17. Test of the "quality" of 1) Delaunay triangulation and 2) TPS interpolations of present-day ungulates hypsodonty in Europe (see figure 14 and text for details).

artefact of the interpolation method (an edge effect) due to a lack of data in high latitudes.

Here, IDL allowed us, through its interpolation methods and visualization facilities, to infer the species richness distribution and the tooth crown height biogeographic patterns of European large mammals. The present-day distribution of species richness produced by the IDL interpolation tool was consistent with previous works (Baquero and Telleria 2001). Regarding ecomorphologic analyses,

hypsodonty was largely related to two climatic parameters (precipitation and temperature) and closely followed a North/South climatic gradient, where the more arid and open environments were to the South. Based on these results, we computed the same ecomorphologic parameter for Tortonian large mammals localities and found out that the North/South broad gradient already existed by late Miocene time.
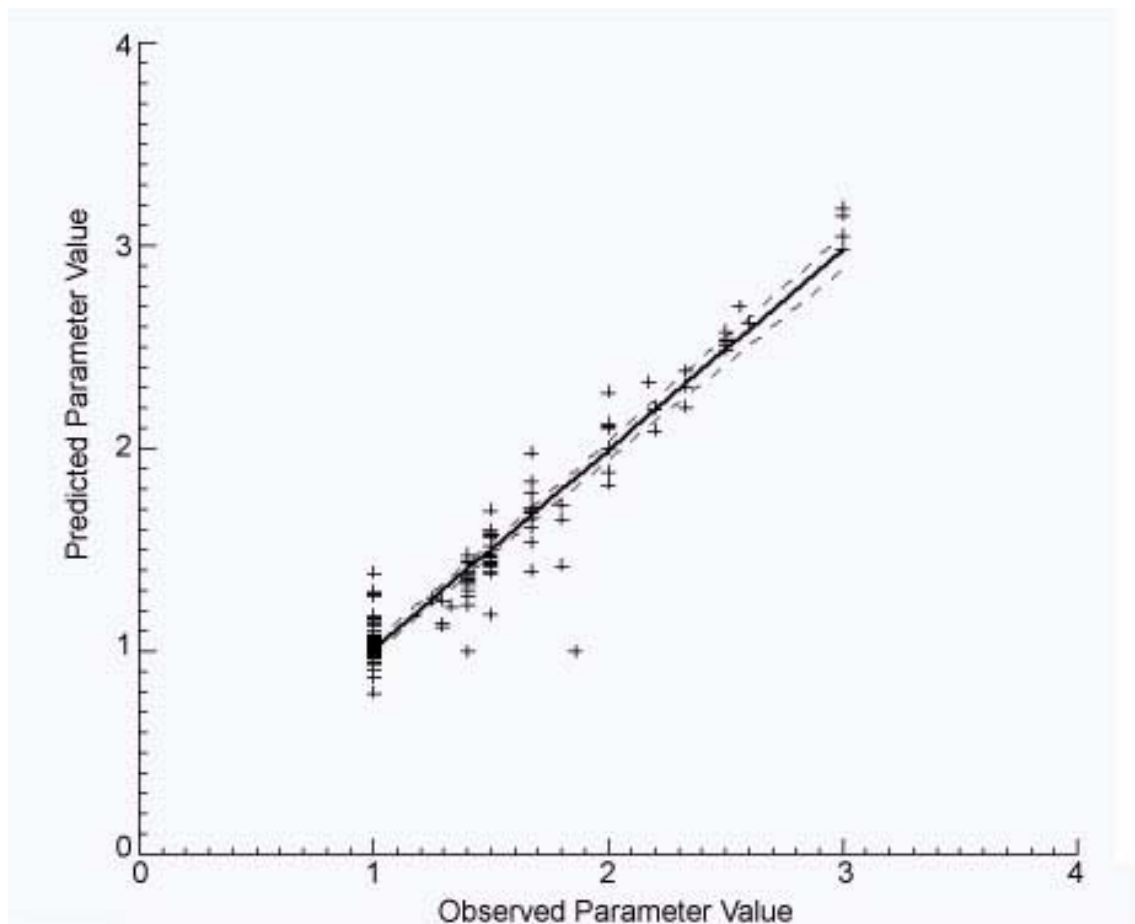
Figure 18. Observed versus TPS-interpolated values; Pearson r = 0.967, bootstrapped (n = 10000) 99% Confidence Interval: 0.93 – 0.99; Mantel's t 0.0001 (n = 10000, H0 = no linear association).

Our fossil map resolution suffers from the low number of localities (100) relative to the large geographic scale taken into account (the whole European continent), as well as from the absence of high latitudes localities due to glacial removal of Miocene continental sediments from northern Europe. Apart from these limitations and the previously discussed problem of spatial heterogeneity, the interpolation methods used in the Tortonian example, especially Delaunay triangulation, seem to produce reliable results.

CONCLUSIONS

We employed IDL to simulate the biodiversity evolution of planktonic species in the Early Triassic and to model biodiversity indices and ecomorphologic parameters for large European Neogene continental mammals.

IDL's flexibility allowed us to generate clear and straightforward visualizations of our results through its large array of pre-packaged routines. Multiple graphic output windows permitted a direct

comparison of complementary results such as the effect of SST and currents on the distribution of Early Triassic ammonoid biodiversity. The creation of customized GIS is facilitated by IDL, and the parameters involved in spatial interpolation of data can easily be monitored in several ways (e.g., spacing of grid points for triangulation and TPS, range of values to be interpolated, interpolated data smoothing, spherical gridding for triangulation). The program routines are easily modified by users for their own purposes.

We used IDL version 5.2, which does not provide all 2-D interpolation methods, limiting the type of data that can be analysed, but it complements more specialized software such as Arcview©, which offers more interpolations but is less capable of importing palaeogeographic maps. In addition, the latest version of IDL (6.0) offers a more convivial user interface as well as improved options, including several additional interpolation methods, further animation possibilities, 3-D reconstruction and auto-executable programs. Thus, with a minimum knowledge of computer programming, this
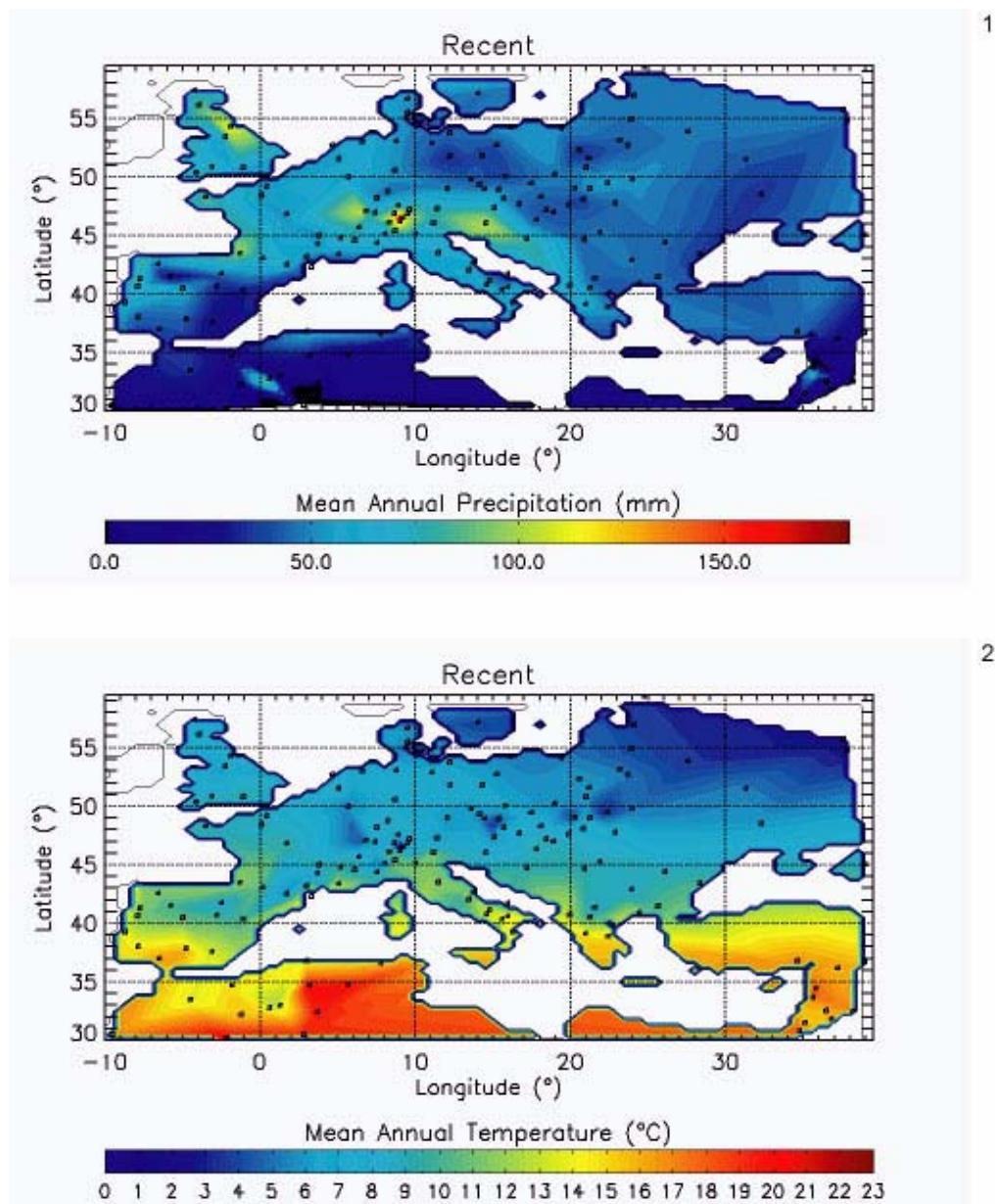
Figure 19. Delaunay triangulated maps for present-day 1) mean annual precipitation, and 2) mean annual temperature. Localities used are shown by open squares; climatic data from LocClim 1.0.

undervalued meta-language offers an array of easily usable tools for a large proportion of palaeontologists.

REFERENCES

Baquero, R., and Telleria, J.L. 2001. Species richness, rarity and endemicity of European mammals: a biogeographical approach. *Biodiversity and Conservation,* 10:29-44.
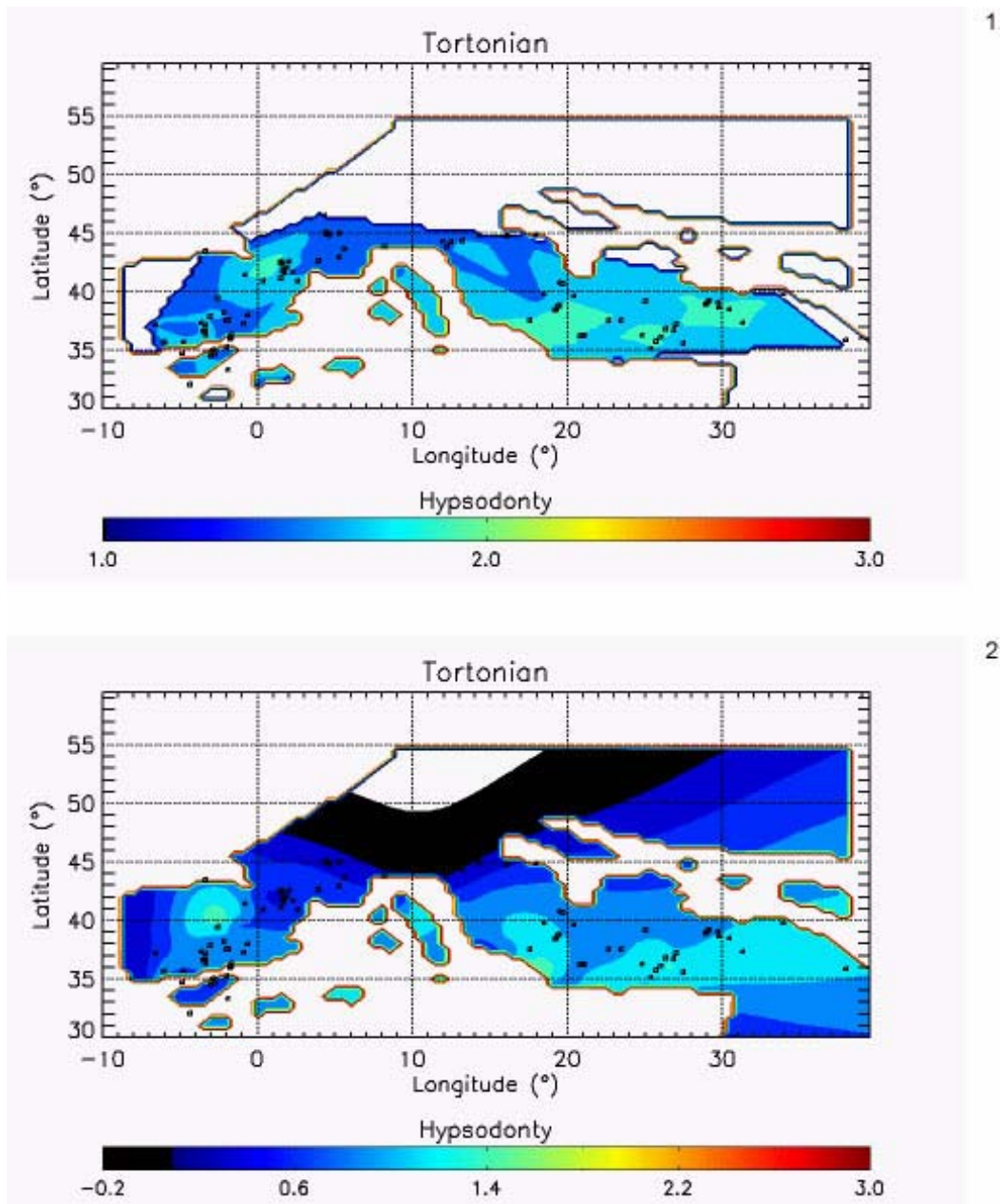
Figure 20. Hypsodonty pattern for 100 European Tortonian sites: 1) Delaunay triangulation interpolation, 2) TPS interpolation. Faunal locations are shown by open squares.

Boer, E.P., de Beurs, K.M., and Hartkamp, A.D. 2001. Kriging and thin plate splines for mapping climate variables. *International Journal of Applied Earth Observation and Geoinformation,* 3:146-154.

Bonis, D.L., Bouvrain, G., Geraads, D., and Koufos, G.D. 1992. Diversity and paleoecology of Greek late Miocene mammalian faunas. *Palaeogeography, Palaeoclimatology, Palaeoecology,* 91:99-121.

Brayard, A. 2002. *Modélisation de l'impact des contraintes climatiques sur la restauration de la biodiversité (sensu Richesse Spécifique) après une crise d'extinction majeure.* Unpublished MSc. Thesis, University Claude Bernard Lyon 1, France.

Casey, R.E. 1989. Model of modern polycystine radiolarian shallow-water zoogeography. *Palaeogeography, Palaeoclimatology, Palaeoecology,* 74:15-22.

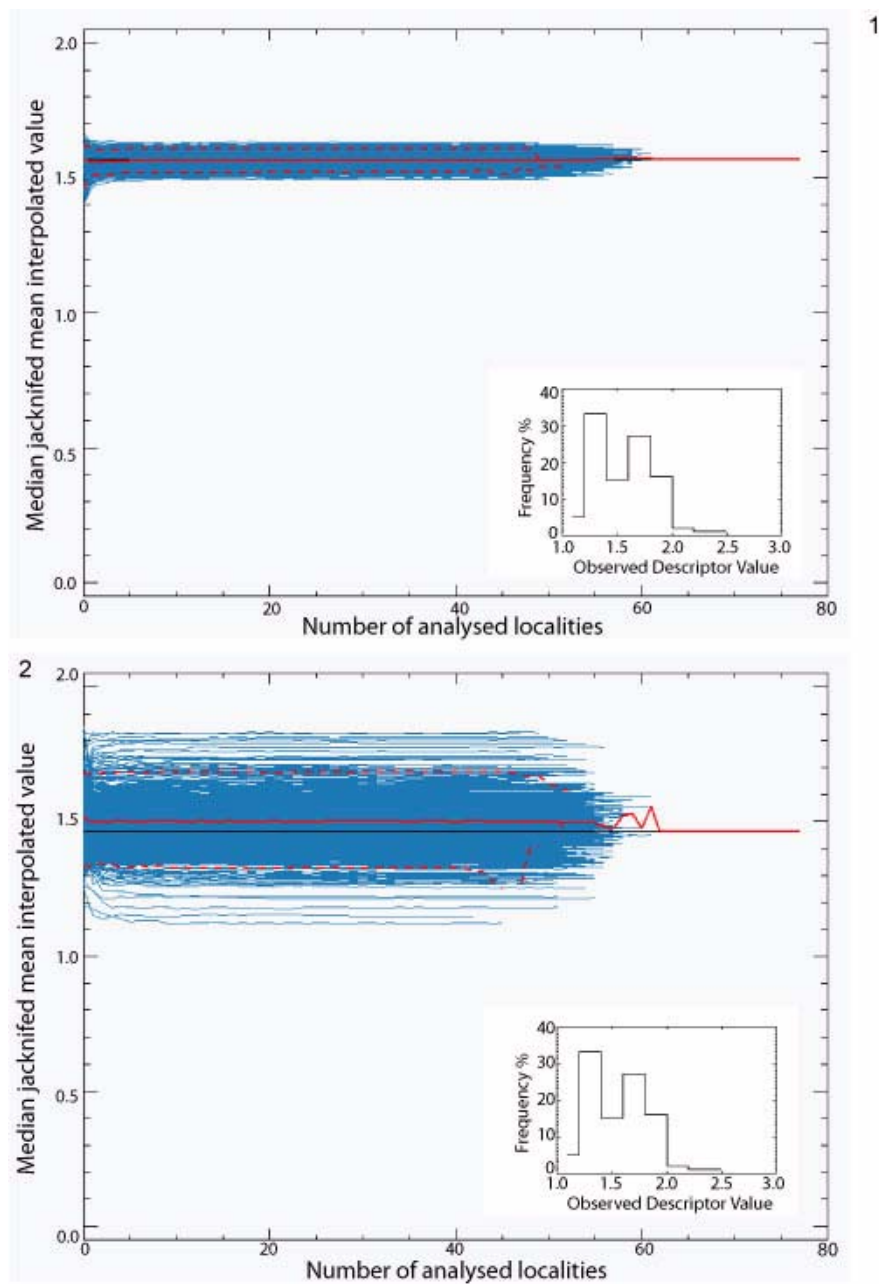Cleland, C.E. 2001. Historical science, experimental science, and the scientific method. *Geology,* 29:987-990.

Figure 21. Test of the "quality" of 1) Delaunay triangulation and 2) TPS interpolations of Tortonian ungulates hypsodonty in Europe (see Figure 14 and text for details).

Colwell, R.K., and Hurtt, G.C. 1994. Nonbiological gradients in species richness and a spurious Rapoport effect. *The American Naturalist,* 144:570-595.

Colwell, R.K., and Lees, D.C. 2000. The mid-domain effect: geometric constraints on the geography of species richness. *Trends in Ecology and Evolution,* 15:70-76.

Colwell, R.K., Rahbek, C., and Gotelli, N.J. 2004. The mid-domain effect and species richness patterns: what have we learned so far? *The American Naturalist,* 163:E1-E23.

Costeur, L., Legendre, S., and Escarguel, G. In press. European large mammals palaeobiogeography and biodiversity from the Early Miocene to the Mid-Pliocene. Palaeogeographic and climatic impacts. *Revue de Paléobiologie, Volume Spécial 9*.

Crame, J.A. 2002. Evolution of taxonomic diversity gradients in the marine realm: a comparison of Late Jurassic and Recent bivalve faunas. *Paleobiology,* 28:184-207.

Dagys, A.S. 1988. Major features of the geographic differentiation of Triassic ammonoids, p. 341-349. In Wiedmann, J., and Kullmann, J. (eds.), *Cephalopods - Present and Past*. Schweizerbart'sche Verlagsbuchhandlung, Stuttgart.
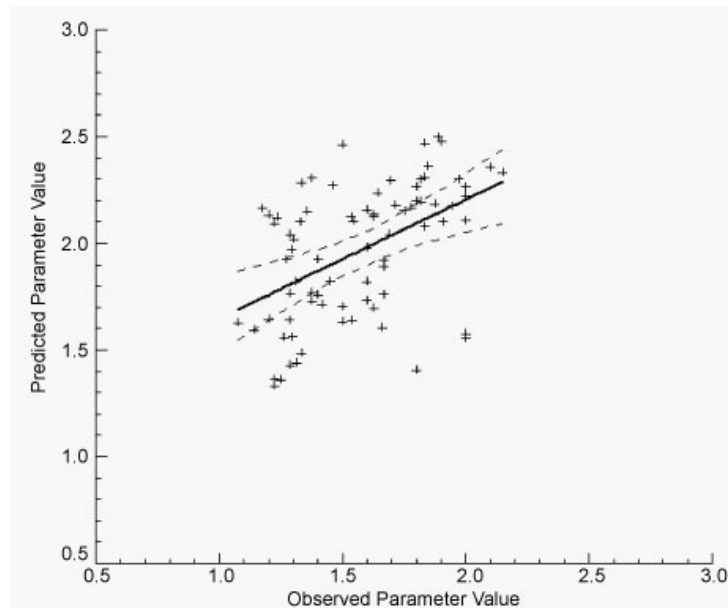
Figure 22. Observed versus TPS-interpolated values; Pearson r = 0.493, bootstrapped (n = 10000) 99% Confidence Interval: 0.21 – 0.70; Mantel's t 0.0001 (n = 10000, H0 = no linear association).

Dagys, A.S. 1997. A new Late Olenekian (Triassic) ammonoid of low paleolatitude affinity from Arctic Asia (Eastern Taimyr). *Paläontologische Zeitschrift,* 71:217-220.

Damuth, J. 1992. Taxon-free characterization of animal communities, p. 183-203. In Behrensmeyer, A.K. et al. (eds.), *Terrestrial Ecosystems through Time.* University of Chicago Press, Chicago.

Elmi, S., and Babin, C. 1996. *Histoire de la Terre.* Masson, Paris.

Erwin, D.H. 1993. *The Great Phanerozoic Crisis: Life and Death in the Permian*, Columbia University Press, New York.

Erwin, D.H. 1994. The Permo-Triassic extinction. *Nature,* 367:231-235.

Erwin, D.H. 1998. The end and the beginning: recoveries from mass extinctions. *Trends in Ecology and Evolution,* 13:344-349.

Erwin, D.H. 2001. Lessons from the past: biotic recoveries from mass extinctions. *Proceedings of the National Academy of Sciences of the United States of America,* 98:5399-5403.

Erwin, D.H., and Pan, H.-Z. 1996. Recoveries and radiations: gastropods after the Permo-Triassic mass extinction, p. 223-229. In Hart, M.B. (ed.), *Biotic Recovery from Mass Extinction Events*. Geological Society Special Publication, Plymouth.

Fortelius, M., Eronen, J., Jernvall, J., Liu, L., Pushkina, D., Rinne, J., Tesakov, A., Vislobokova, I., Zhang, Z., and Zhou, L. 2002. Fossil mammals resolve regional patterns of Eurasian climate change over 20 million years. *Evolutionary Ecology Research,* 4:1005-1016.

Fortelius, M., and Solounias, N. 2000. Functional characterization of ungulate molars using the abrasion-attrition wear gradient: a new method for reconstructing paleodiets. *American Museum Novitates,* 3301:1-36.

Fortelius, M., Werdelin, L., Andrews, P., Bernor, R.L., Gentry, A., Humphrey, L., Mittman, H.-W., and Viratana, S. 1996. Provinciality, diversity, turnover, and paleoecology in land mammals faunas of the later Miocene of Western Eurasia, p. 414-448. In Bernor, R.L., Fahlbush, V., and Mittman, H.-W. (eds.), *The Evolution of Western Eurasian Neogene Mammals Faunas.* Columbia University Press, New York.

Gaston, K.J. 2000. Global patterns in biodiversity. *Nature,* 405:220-227.

Hotinski, R.M., Bice, K.L., Kump, L.R., Najjar, R.G., and Arthur, M.A. 2001. Ocean stagnation and end-Permian anoxia. *Geology,* 29:7-10.

Jernvall, J., and Fortelius, M. 2002. Common mammals drive the evolutionary increase of hypsodonty in the Neogene. *Nature,* 417:538-540.

Kidder, D.L., and Worsley, T.R. 2004. Causes and consequences of extreme Permo-Triassic warming to globally equable climate and relation to Permo-Triassic extinction and recovery. *Palaeogeography, Palaeoclimatology, Palaeoecology,* 203:207-237.

Kiessling, W. 2002. Radiolarian diversity patterns in the latest Jurassic-earliest Cretaceous. *Palaeogeography, Palaeoclimatology, Palaeoecology,* 187:179-206.

Kummel, B. 1973. Aspects of the Lower Triassic (Scythian) stage, p. 557-571. In Logan, A., and Hills, L.V. (eds.), *The Permian and the Triassic Systems and Their Mutual Boundary*. Canadian Society of Petroleum Geologists, Calgary.

Legendre, S. 1989. Les communautés de mammifères du Paléogène (Eocène supérieur et Oligocène) d'Europe occidentale: structure, milieux et évolution. *Müncher Geowissenschaftliche Abhandlungen (A),* 16:1-110.

LocClim1.0 2002. Environment and natural resources working paper 9 (CD-ROM). Supplied by the Food and Agriculture Organization of the United Nations.

Marschallinger, R. 2001. Three-dimensional reconstruction and visualization of geological materials with IDL - examples and source code. *Computers and Geosciences,* 27:419-426.

Meulenkamp, J.E., and Sissingh, W. 2003. Tertiary palaeogeography and tectonostratigraphic evolution of the northern and southern Peri-Tethys platforms and the intermediate domains of the African-Eurasian convergent plate boundary zone. *Palaeogeography, Palaeoclimatology, Palaeoecology,* 196:209-228.

Monnet, C., Bouchet, S., and Thiry-Bastien, P. 2003. ISOPAQ, a MATLAB program for stratigraphic and isopach mapping: example application to the French Bajocian (Jurassic) sediments. *Computers and Geosciences,* 29:1101-1110.

Pickard, G.L., and Emery, W.J. 1990. *Descriptive Physical Oceanography: An Introduction.* Pergamon Press, Oxford.

Raup, D.M., and Sepkoski, J.J. 1982. Mass extinctions in the marine fossil record. *Science,* 215:1501-1503.

Rex, M.A., Stuart, C.T., Hessler, R.R., Allen, J.A., Sanders, H.L., and Wilson, G.D.F. 1993. Global-scale latitudinal patterns of species diversity in the deep-sea benthos. *Nature,* 365:636-639.

Rögl, F. 1999. Mediterranean and Paratethys paleogeography during the Oligocene and Miocene, p. 8-22. In Agusti, J., Rook, L., and Andrews, P. (eds.), *Hominoid Evolution and Climatic Change in Europe. Volume 1. The Evolution of Neogene Terrestrial Ecosystem in Europe.* Cambridge University Press, Cambridge.

Rhodes, K. 1992. Latitudinal gradients in species diversity: the search for the primary cause. *Oikos,* 65:514-527.

Rutherford, S., D'Hondt, S., and Prell, W. 1999. Environmental controls on the geographic distribution of zooplankton diversity. *Nature,* 400:749-753.

Schopf, T.J.M. 1970. Taxonomic diversity gradients of ectoprocts and bivalves and their geologic implications. *Geological Society of America Bulletin,* 81:3765-3768.

Smith, A.G., Smith, D.G., and Funnell, B.M. 1994. *Atlas of Mesozoic and Cenozoic Coastlines.* Cambridge University Press, Cambridge.

Stehli, F.G., Douglas, R.G., and Newell, N.D. 1969. Generation and maintenance of gradients in taxonomic diversity. *Science,* 164:947-949.

Sugihara, K. and Inagaki, H., 1995. Why is the 3D Delaunay triangulation difficult to construct? *Information Processing Letters,* 54: 275-280.

Tozer, E.T. 1973. The earliest marine Triassic rocks: their definition, ammonoid fauna, distribution and relationship to underlying formations, p. 549-556. In Logan, A., and Hills, L.V. (eds.), *Permian and Triassic Systems and their Mutual Boundary.* Canadian Society of Petroleum Geologists, Calgary.

Tozer, E.T. 1994. Canadian Triassic ammonoid faunas. *Geologic Survey of Canada Bulletin,* 467:1-663.

Van Dam, J., and Weltje, G.J. 1999. Reconstruction of the Late Miocene climate of Spain using rodent palaeocommunity successions: an application of end-member modelling. *Palaeogeography, Palaeoclimatology, Palaeoecology,* 151:267-305.

Wootton, T.J. 2001. Local interactions predict large-scale pattern in empirically derived cellular automata. *Nature,* 413:841-844.

Yu, Z.W. 2001. Surface interpolation from irregularly distributed points using surface splines, from Fortran program. *Computers and Geosciences,* 27:877-882.